

Hunanamycin A, an Antibiotic from a Marine-Derived *Bacillus hunanensis*

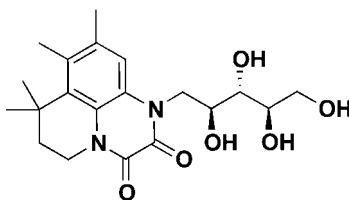
Youcai Hu, Kezhan Wang, and John B. MacMillan*

Department of Biochemistry, University of Texas Southwestern Medical Center at Dallas, Dallas, Texas 75390, United States

john.macmillan@utsouthwestern.edu

Received December 10, 2012

ABSTRACT



Hunanamycin A, the first natural product with a pyrido[1,2,3-*de*]quinoxaline-2,3-dione core, was isolated from a marine-derived *Bacillus hunanensis*. Hunanamycin A is related to a degradation product of riboflavin but has undergone an N-prenylation and subsequent cyclization. The structure, including stereochemistry, was determined by NMR and MS methods. Hunanamycin A exhibits a minimum inhibitory concentration (MIC) of 12.4 μ M against the bacterial pathogen *Salmonella enterica*.

Riboflavin plays an essential role in the metabolism of most organisms.¹ While humans and other animals obtain riboflavin from their diet, a variety of Gram-negative bacteria and certain yeasts lack an efficient uptake system and therefore require endogenous production.² Riboflavin synthase catalyzes the final step in the biosynthesis of riboflavin (Figure 1), converting 2 equiv of 6,7-dimethyl-8-D-riboityllumazine (**1**) into riboflavin (**2**) and 5-amino-6-D-riboitylamino-2,4-(1*H*,3*H*)-pyrimidinedione (**3**) (Figure 1). Since humans lack riboflavin synthase, it has been shown to be an attractive antibiotic target, specific for certain Enterobacteria (such as *E. coli*, *Salmonella*) and yeasts.³ In disease models of *Salmonella* infection, knockout of the riboflavin synthase *ribB* was shown to be lethal to the pathogen.⁴

Based on insights from the X-ray crystal structures of riboflavin synthases, there have been a number of studies toward the rational design of inhibitors, such as a class of 6-phosphonoxyalkyl derivatives of 7-oxo-8-riboitylamino-lumazine and 9-D-riboitylamino-1,3,7,9-tetrahydro-2,6,

8-purinetriones bearing alkyl phosphate substituents.^{5,6} Although these molecules showed μ M inhibition of riboflavin synthase, they have no *in vivo* activity against pathogens, which has been attributed to their inability to penetrate microbial cells.⁵

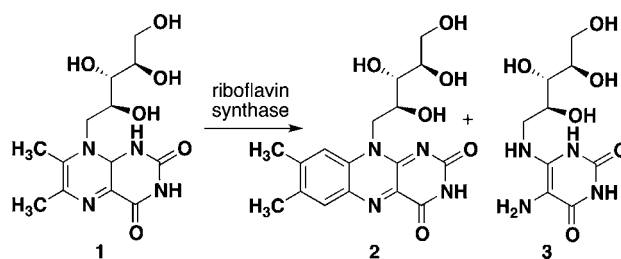


Figure 1. Biochemical transformation of riboflavin synthase.

(1) Henriques, B. J.; Rikke, K. O.; Bross, P.; Gomes, C. M. *Curr. Med. Chem.* **2010**, *17*, 3842–3854.

(2) Illarionov, B.; Eisenreich, W.; Bacher, A. *Proc. Natl. Acad. Sci. U. S. A.* **2001**, *98*, 7224–7229.

(3) Mortl, S.; Fischer, M.; Richter, G.; Tack, J.; Weinkauff, S.; Bacher, A. *J. Biol. Chem.* **1996**, *271*, 33201–33207.

(4) Rollenhagen, C.; Bumann, D. *Infect. Immun.* **2006**, *74*, 1649–1660.

(5) Kaiser, J.; Illarionov, B.; Rohdich, F.; Eisenreich, W.; Saller, S.; Van den Brulle, J.; Cushman, M.; Bacher, A.; Fischer, M. *Anal. Biochem.* **2007**, *365*, 52–61.

(6) (a) Zhang, Y.; Jin, G.; Illarionov, B.; Bacher, A.; Fischer, M.; Cushman, M. *J. Org. Chem.* **2007**, *72*, 7176–7184. (b) Ramsperger, A.; Augustin, M.; Schott, A. K.; Gerhardt, S.; Krojer, T.; Eisenreich, W.; Illarionov, B.; Cushman, M.; Bacher, A.; Huber, R.; Fischer, M. *J. Biol. Chem.* **2006**, *281*, 1224–1232. (c) Cushman, M.; Jin, G.; Illarionov, B.; Fischer, M.; Ladenstein, R.; Bacher, A. *J. Org. Chem.* **2005**, *70*, 8162–8170.

During the course of biological and chemical studies of *Bacillus humanensis* strain SNA-048 for molecules with selective cytotoxicity against nonsmall cell lung cancer (NSCLC) cell lines,⁷ we came across a molecule that had structural features of riboflavin but, based on the molecular weight, UV profile, and NMR signals, was determined to be the novel compound hunanamycin A (**4**), which is the first example of a *N*-prenylated riboflavin analog. Based on the structural resemblance of **4** to the synthetic inhibitors of riboflavin synthase^{6c} (Figure 2), we evaluated the ability of **4** to inhibit growth of the riboflavin synthase dependent bacteria *Salmonella enterica* as well as three additional bacteria. Herein we report the structural and biological characterization of **4**.

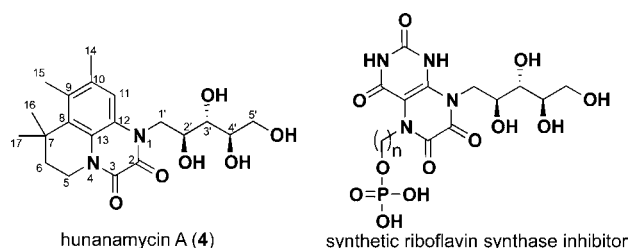


Figure 2. **1** and synthetic riboflavin synthase inhibitors.

Marine bacterium SNA-048 was isolated from a sediment sample collected from a mangrove swamp in the Bahamas and isolated on an acidified Gauze media. Analysis of the strain by 16S rRNA revealed a 98% identity to *Bacillus humanensis*.⁸ A large-scale fermentation (120 L) by shake fermentation was carried out to obtain sufficient material for full chemical and biological analysis of the new compounds. The excreted metabolites were collected using XAD-7 resin, and the resulting crude extract was purified by a combination of solvent/solvent extraction (*n*-hexane, DCM, and methanol/H₂O) and reversed phase chromatography to give multiple fractions. Final purification by gradient reversed-phase HPLC gave hunanamycin A (**4**, 0.8 mg).

Hunanamycin A (**4**) was isolated as a light yellow glass; high-resolution ESI-MS (HRESIMS) analysis of **4** gave an $[M + H]^+$ at m/z 393.2018 consistent with a molecular formula of C₂₀H₂₈N₂O₆ (calcd for C₂₀H₂₉N₂O₆, 393.2025) and 8 degrees of unsaturation.

The ¹H, ¹³C, and HSQC NMR spectra of **4** (Table 1) showed the presence of a pentasubstituted benzene ring suggested by a single aromatic proton at δ_H 7.47 (s, H-11) and six aromatic carbons at δ_C 136.0, 134.3, 133.8, 126.2,

123.3, and 117.2; three oxygenated methines (C-2'–C-4', δ_H 4.25/ δ_C 70.6, δ_H 3.76/ δ_C 75.0, and δ_H 3.77/ δ_C 74.4); one oxygenated methylene (C-5', δ_H 3.81, 3.67/ δ_C 65.0); three methylenes (C-5, C-6, and C-1', δ_H 4.12/ δ_C 39.3, δ_H 4.79, 4.28/ δ_C 46.6, and δ_H 1.94/ δ_C 40.8); four methyls (C-14–C-17, δ_H 2.33/ δ_C 21.6, δ_H 2.45/ δ_C 19.6, δ_H 1.55/ δ_C 29.3, and δ_H 1.54/ δ_C 29.0); two downfield quaternary carbons at δ_C 156.7 and 155.3; and one upfield quaternary carbon at δ_C 34.5 (C-7).

The pentasubstituted benzene ring was deduced by analysis of the gHMBC spectrum (Figure 3). The aromatic proton at δ_H 7.47 showed strong HMBC correlations with three carbons at δ_C 133.8 (C-9), 21.6 (C-14), and 123.3 and weak correlations with two carbons at δ_C 136.0 (C-10) and 126.2 (C-12), and the methyl at δ_H 2.33 (H-14) showed HMBC correlations with C-11 (δ_C 117.2), C-10, and C-9, while the methyl at δ_H 2.45 (H-15) had HMBC correlations with C-10, C-9, and C-8 (δ_C 134.3). These HMBC correlations not only clearly assigned the chemical shifts of C-8–C-13 but also placed methyl substituents at C-9 and C-10 of the aryl ring.

Table 1. 1D and 2D NMR Data for **4** in CD₃OD

no.	δ_H , mult. (<i>J</i> in Hz)	δ_C	COSY	HMBC
2		156.7		
3		155.3		
5	4.12, m	39.3	6	3, 6, 7, 13
6	1.94, t (5.9)	40.8	5	5, 7, 8, 16, 17
7		34.5		
8		134.3		
9		133.8		
10		136.0		
11	7.47, s	117.2	14	9, 10, 12, 13 14
12		126.2		
13		123.3		
14	2.33, s	21.6		9, 10, 11
15	2.45, s	19.6		8, 9, 10
16	1.55, s	29.3		6, 7, 8, 17
17	1.54, s	29.0		6, 7, 8, 16
1'α	4.79, dd (9.8, 14.3)	46.6	1'β, 2	2, 12, 2', 3'
1'β	4.28, dd (2.9, 14.3)		1'α, 2	2, 12
2'	4.25, ddd (9.9, 2.9, 4.0)	70.6	1', 3'	1'
3'	3.76, dd (4.0, 7.2)	75.0	2'	1', 4'
4'	3.77, ddd (7.2, 5.0, 2.9)	74.4	5'	2', 3', 5'
5'α	3.81, dd (2.9, 11.2)	65.0	5'β	3'
5'β	3.67, dd (5.0, 11.2)		4', 5'α	3', 4'

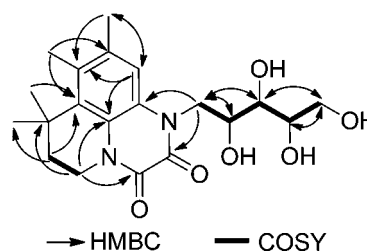


Figure 3. Key correlations for structural assignment of **4**.

(7) Potts, M. B.; Kim, Y.; Fisher, K. W.; Hu, Y.; Carrasco, Y.; Ou, Y.-H.; Herrera, M.; Cubillos, F.; Xiao, G.; Hofree, M.; Ideker, T.; Xie, Y.; Lewis, R. E.; MacMillan, J. B.; White, M. A. *Science* **2012** in revision.

(8) Genomic DNA of strain SNA-048 was isolated using standard methods and was amplified using PCR with the Universal 16S rRNA primers FC27 and RC 1492. The partial 16S rRNA sequence of 1472 bp was compared to sequences in available databases using the Basic Local Alignment Search Tool and strain SNA-048 determined to be 98% similar to *Bacillus humanensis*. The 16S rRNA sequence of SNA-048 was deposited in the GenBank, accession no. KC247801.

The presence of an isopentyl group was suggested by a COSY correlation between H-5 (δ_{H} 4.12) and H-6 (δ_{H} 1.94) and HMBC correlations from H-6 to C-5, C-7, C-16, and C-17, as well as from H-5 to C-6 and C-7. HMBC correlations from H-6 and the two methyl groups (H-16 and H-17) to the aromatic carbon C-8 indicated the direct connection between C-7 and C-8. The chemical shift of H-5 (δ_{H} 4.12) and C-5 (δ_{C} 39.3) highly suggested C-5 was substituted by a nitrogen atom. An HMBC correlation from H-5 to C-13 indicated that C-5 was connected to C-13 by a nitrogen atom (N-4). The downfield shift of the C-6 methylene to 40.8 is most likely due to shielding by the geminal dimethyl substituent and is consistent with literature values for similar ring systems.⁹

The presence of a pentitol was indicated by ^1H , ^{13}C NMR and COSY spectra and confirmed by HMBC correlations. The chemical shifts of H-1' (δ_{H} 4.79 and 4.28)^{6c} and C-1' (δ_{C} 46.6) and the HMBC correlation from H-1' to C-12 indicated that C-1' was connected to C-12 through another nitrogen atom (N-1).

The remaining substructure accounts for C_2O_2 and 3 degrees of unsaturation. The chemical shift of the two remaining downfield quaternary carbons at δ_{C} 155.3 (C-3) and δ_{C} 156.7 (C-2) and HMBC correlations from H-1' to C-2 and from H-5 to C-3 indicated the functionality of the two carbons as amides. To fulfill the 8 degrees of unsaturation, it required an additional ring in **4**, which indicated the direct connection of C-2 and C-3. The chemical shifts for the two amides are further upfield than normal; however they are consistent with synthetic analogs with similar ring systems.^{6c,10} As a result, the assignment of the entire backbone of **4** was completed. **4** represented the first natural product with a pyrido[1,2,3-*de*]quinoxaline-2,3-dione core.

The relative configuration of **4** was assigned by the coupling constants of H-1'–H-5' and NOE correlations (Figure 4). Thorough studies on the conformation of various 1-amino-1-deoxy-pentitol derivatives by Horton and co-workers has provided valuable data for assigning the relative configuration of such moieties.¹¹ These studies demonstrated for example that the *D-arabino*- and *D-lyxo*-isomers adopt extended, planar, zigzag conformations, whereas the *D-xylo*- and *D-ribo*-isomers have the carbon chain in a nonplanar, “sickle” arrangement. Based on their experimental evidence, the 1-amino-1-deoxy-*D*-ribitol configuration is oriented such that there is a small $^3J_{\text{H}_2\text{H}_3}$ and a large $^3J_{\text{H}_3\text{H}_4}$. This leads to a rotation about C-2–C-3 to adopt the sickle conformer (${}_2G^-$) to eliminate the 1,3-interaction between C-1 and O-3.¹¹ However, these data are all recorded in D_2O or $\text{DMSO}-d_6$, which was limiting for **4** due to insolubility and spectral overlap. However, we

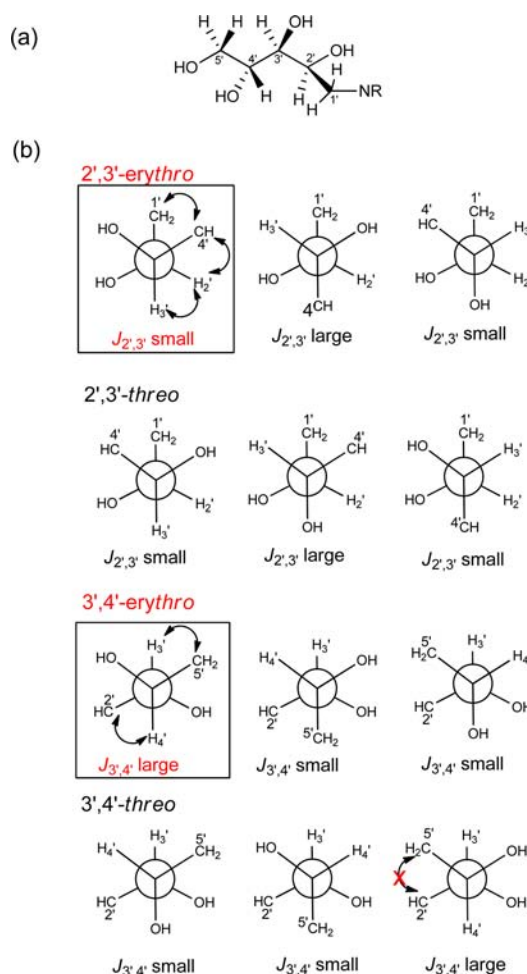


Figure 4. (a) Conformation of ribo-isomer; (b) Stereochemistry of C-2', C-3', and C-4' in **4**. Box indicates conformation that agrees with measured data.

were able to utilize some aspects of the configurations to provide evidence for the *D-ribo* configuration of **4**.

The small coupling constant between H-2' and H-3' ($J = 4.0$ Hz) and a large coupling constant between H-3' and H-4' ($J = 7.2$ Hz)¹² in **4** match with the reported values for 1-amino-1-deoxy-*D*-ribitol derivatives, indicating the *erythro* configuration for both 2',3' and 3',4' in **4** (Figure 4). As described below, it is most likely that **4** is derived from catabolism of riboflavin, which contains a *D*-configured ribitol, consistent with the coupling values described above. Direct comparison of $^3J_{\text{HH}}$ and ^{13}C chemical shifts of the tetraol moiety of **4** with those of riboflavin measured in the same solvent (both CD_3OD and $\text{DMSO}-d_6$) showed almost identical data (Figure 5; Figure S1; Tables S2, S3). In particular the couplings between H2'/H3' and H3'/H4' are identical between **2** and **4**. As such, it is most likely that

(9) Atwal, K. S.; Ferrara, F. N.; Ding, C. Z.; Grover, G. J.; Sleph, P. G.; Dzwonczyk, S.; Baird, A. J.; Normandin, D. E. *J. Med. Chem.* **1996**, *39*, 304–313.

(10) (a) Ooike, M.; Nozawa, K.; Kawai, K.-I. *Phytochemistry* **1997**, *46*, 123–126. (b) Overman, L. E.; Shin, Y. *Org. Lett.* **2007**, *9*, 339–341.

(11) (a) Blanc-Muesser, M.; Defaye, J.; Horton, D. *Carbohydr. Res.* **1979**, *68*, 175–187. (b) Horton, D.; Thomas, S.; Gallucci, J. *Carbohydr. Res.* **2006**, *341*, 2211–2218. (c) Vejcek, S. M.; Horton, D. *Carbohydr. Res.* **2007**, *342*, 806–818.

(12) The coupling constant between H-2' and H-3' was easily obtained from the H-2' multiplet; however due to overlap of H-3' and H-4' in the ^1H NMR at 22 °C, it was not possible to obtain coupling values. Acquisition of the ^1H NMR at 45 °C provided resolution of the H-3' and H-4' signals, providing measurable coupling values.

the ribitol substituent in **4** is of the D-configuration and the absolute configuration is 2',3',4' R.

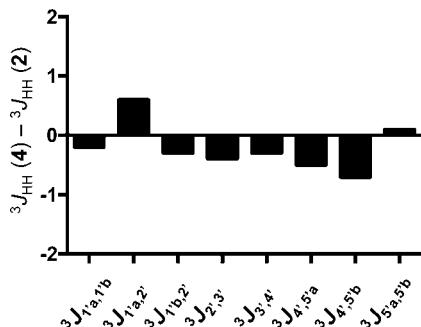


Figure 5. Comparison of $^3J_{\text{HH}}$ of **4** and **2** in CD_3OD .

The relative configuration assignment was also supported by data obtained from a 2D ROESY experiment. The NOE correlations of H-2'/H-3', H-2'/H-4', H-3'/H-5', and H-1'/H-4' supported the 2',3'-erythro configuration (Figure 4b), while the presence of NOE correlations of H-2'/H-4' and H-1'/H-3' and the absence of an NOE correlation between H-2'/H-5' supported the 3',4'-erythro configuration. However, due to the similar chemical shifts of H3' and H4', unambiguous NOE assignments are limited.

The structurally closest compound of **4** in the literature is 1-ribityl-2,3-diketo-1,2,3,4-tetrahydro-6,7-dimethyl-quinoxaline (**5**)¹³ which was from an unnamed soil bacteria as a degradation product of riboflavin (**2**). We envisage a biosynthetic pathway where *N*-prenylation of a degradation intermediate such as **6**, followed by electrophilic attack on the aromatic carbon by the π -system in the prenyl unit in a manner similar to a Friedel–Crafts alkylation, would give rise to **4** (Figure 6).

Based on the structure we predicted that **4** would be an inhibitor of riboflavin synthase and therefore would have antimicrobial activity against bacterial strains that lacked riboflavin transport mechanisms. We pursued the

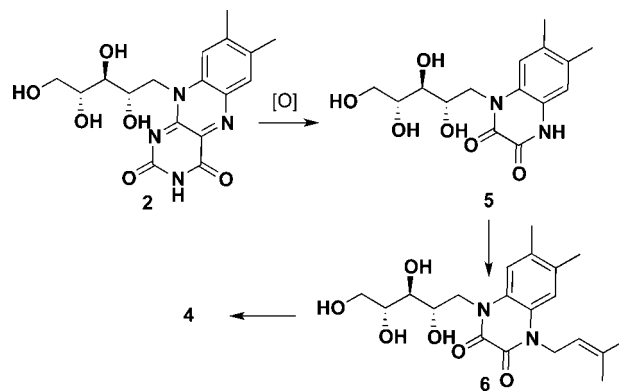


Figure 6. Proposed biosynthetic pathway of **4**.

antimicrobial activity against *Salmonella enterica*, *Mycobacterium smegmatis*, *Bacillus subtilis*, and *Pseudomonas aeruginosa*. Of the four bacteria, only *Salmonella enterica* lacks efficient mechanisms for exogenous uptake of riboflavin. The MIC of **4** against *S. enterica* was found to be $12.4 \mu\text{M}$, while there was no effect against *M. smegmatis*, *B. subtilis*, or *P. aeruginosa* at concentrations $< 100 \mu\text{M}$. Although this does not confirm that **4** is an inhibitor of riboflavin synthase, it is suggestive. Further evaluation of the compound is needed using *in vitro* assays for riboflavin synthase inhibition. Although an MIC of $12.4 \mu\text{M}$ is not an extremely potent antibiotic, the selectivity for *S. enterica* makes this a promising lead for further studies.

Acknowledgment. We thank Mark Cushman (Purdue University) for suggesting the possibility this compound is an inhibitor of riboflavin synthase. We acknowledge the following grants for funding this project: Welch Foundation I-1689. J.B.M. is a Chilton/Bell Foundation Endowed Scholar.

Supporting Information Available. General procedures, bioassay protocols, data tables, and NMR spectra. This material is available free of charge via the Internet at <http://pubs.acs.org>.

The authors declare no competing financial interest.

(13) Todd Miles, H.; Smyrniotis, P. Z.; Stadtman, E. R. *J. Am. Chem. Soc.* **1959**, *81*, 1946–1951. (b) Harkness, D. R.; Stadtman, E. R. *J. Biol. Chem.* **1965**, *240*, 4089–4096.